52.0 – L DATA DRIVEN QUALIFICATION (DDQ) FRAMEWORK FOR METALS ADDITIVE MANUFACTURING

Charles Smith (Mines)
Faculty: Jonah Klemm-Toole (Mines) and Amy Clarke (Mines)
Participant: Craig Brice (Mines)
Sponsor: National Center for Defense Manufacturing and Machining

This project was initiated in January 2021 by the National Center for Defense Manufacturing and Machining. The research performed during this project will serve as the basis for a Master's thesis program for Charles Smith.

52.1 Project Overview and Industrial Relevance

This project aims to solve an inherent problem with additive manufacturing systems. The range of equipment suppliers that use their proprietary feedstock and process parameters makes each AM system and qualification protocol unique. This creates a lengthy qualification process for any new part or material used in manufacturing. This project uses a data-driven qualification approach from relationships across platforms and alloy systems using intelligent machine learning algorithms and physics-based modeling. This project aims to create relationships between solidification velocity, thermal gradients, and microstructure development to help accelerate the qualification and adoption of additive manufactured parts into defense application.

52.2 Previous Work

316L stainless steel was previously acquired as the sponsor specified material for this project. 316L stainless steel exhibits unique solidification behavior where the primary solidifying phase changes with increasing solidification velocity. Based on the phase diagram, one might assume that 316L would likely experience primary delta ferrite solidification with a solid-state phase transformation into gamma austenite as the material cools. However, in processes that experience fast solidification, such as laser powder bed fusion (LPBF), the primary solidification changes to primary austenite solidification, resulting in a microstructure that contains little to no ferrite in the cooled part [52.1]. This change usually results in increased residual stress in the as-built LPBF material and can lead to solidification cracking. Also, the composition range 316L stainless steel is characterized as is quite extensive and lies in a region where slight variations in compositions can change the solidification behavior [52.2].

Process parameters of LPBF significantly influence the properties of the as-built material by influencing thermal gradients and solidification behavior. An analytical method to determine ideal process parameters is to use a volumetric energy calculation**, Equation 52.1**. This equation uses laser power (P), scan speed (v), hatch distance (h), and layer thickness (l) to determine the total energy (E_d) the build is exposed to during the LPBF process [52.3]. Results in the literature suggest that the ideal volumetric energy value is in the range of 100 – 105 $\frac{J}{mm^3}$ [52.4]. Materials that are processed using lower values would be more likely to experience increases in porosity, while higher values are likely to experience lower hardness values in the as-built condition [52.4].

$$E_d = \frac{P}{v*h*l} \tag{52.1}$$

Previous work has focused on the development of defect maps that indicate where particular solidification behavior emerges as shown in Figure 52.1. These maps use process parameters to predict when balling, keyholing, and lack of fusion occur for 316L stainless steel. The Rosenthal model was used to predict the melt pool geometry from process parameters, and geometrical features were combined with analytical models for these defects to generate the map. These maps give approximate values for the occurrence of these defects, but the predictive capability is limited by the assumptions inherent in Rosenthal model [52.5].

52.3 Recent Progress

52.3.1 Microstructure Analysis of 316L LPBF Builds

Microstructure analysis of 316L LPBF builds has begun. The goal of the first build, shown in Figure 52.2, is to determine the effects that part sizes and proximity of nearby builds have on the as-built microstructure. The build was generated using parameters given by 3D Systems for the Mines DMP Flex 350 equipment and serves as a baseline for the project. Each plate was sectioned at the beginning, middle, and end of the length of the plate, and microstructures were observed along the build height in these sections. Scanning electron microscopy (SEM), electron backscattered diffraction (EBSD) and energy dispersive spectroscopy (EDS) have begun to assess any systematic changes in the microstructure as a function of location within the build. The melt pool dimensions will be compared against predictions from the Rosenthal model. Dendrite arm spacing and grain morphology will also be experimentally evaluated and compared against predictions from solidification models.

52.3.2 Abaqus Simulations of Moving Heat Source

This project aims to predict microstructure from thermal gradients (G) and solidification velocities (V) during LPBF. Ideally, thermal gradients could be measured during LPBF processing. However, due to the small scale of the melt pool and high travel speeds, such measurements are not currently possible. Accordingly, thermal simulations are the only way to determine G and V at all points in the solid liquid interface during solidification. Abaqus was chosen for this role due to its flexibility and adaptability, allowing the same simulation to be systematically changed to represent different rostering paths and printing techniques. These simulations are done to represent a single moving heat source across a piece of 316L stainless steel, as shown in Figure 52.3. Further analysis has started by observing temperatures at predetermined nodes to calculate G and V from the simulations as indicated in Figure 52.4.

52.4 Plans for Next Reporting Period

The goals for the next reporting period are as follows:

- Continue work on the Abaqus simulations to be able to adapt to more complex printing processes.
- Continue analysis of the Abaqus simulation to calculate G and V for a given simulation.
- Continue work on the microstructure analysis of the 316L builds.
- Start work on other simulation platforms and techniques to be used as a comparison to the Abaqus simulations.
- Start determining process parameter sets to make connections between thermal gradients and solidification velocity changes to the as-built microstructure.

52.5 References

[1] S.A. David, J.M. Vitek, T.L. Hebble, Effect of Rapid Solidification on Stainless Steel Weld Metal Microstructures and Its Implications on the Schaeffler Diagram., Weld. J. (Miami, Fla). 66 (1987). https://doi.org/10.2172/5957599.

[2] J. LIPPOLD, Solidification behavior and cracking susceptibility of pulsed-laser welds in austenitic stainless steels, Weld. J. 73 (1994) 129.

[3] M. Zhang, C.N. Sun, X. Zhang, P.C. Goh, J. Wei, D. Hardacre, H. Li, Fatigue and fracture behaviour of laser powder bed fusion stainless steel 316L: Influence of processing parameters, Mater. Sci. Eng. A. 703 (2017) 251–261. https://doi.org/10.1016/j.msea.2017.07.071.

[4] A. Leicht, M. Rashidi, U. Klement, E. Hryha, Effect of process parameters on the microstructure, tensile strength and productivity of 316L parts produced by laser powder bed fusion, Mater. Charact. 159 (2020) 110016. https://doi.org/10.1016/j.matchar.2019.110016.

[5] J.N. Zhu, E. Borisov, X. Liang, E. Farber, M.J.M. Hermans, V.A. Popovich, Predictive analytical modelling and experimental validation of processing maps in additive manufacturing of nitinol alloys, Addit. Manuf. 38 (2021) 101802. https://doi.org/10.1016/j.addma.2020.101802.

52.6 Figures and Tables

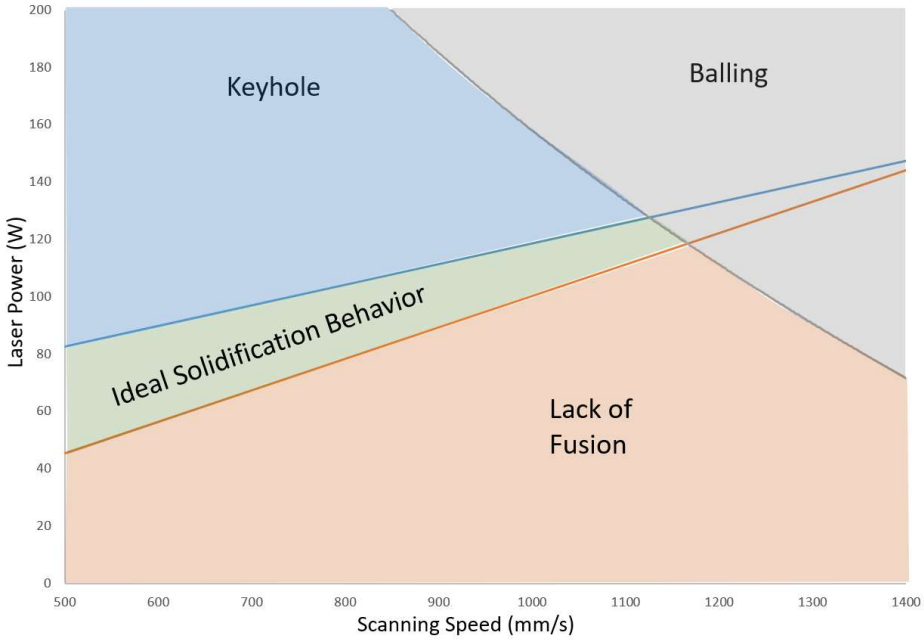

Figure 52.1: Defect map of an LPBF process of 316L stainless steel with a laser spot size of 0.1mm, a hatch distance of 0.1mm, and a layer thickness of 0.04mm. The highlighted areas show where keyholing, balling, and lack of fusion occur along with ideal solidification behaviors.

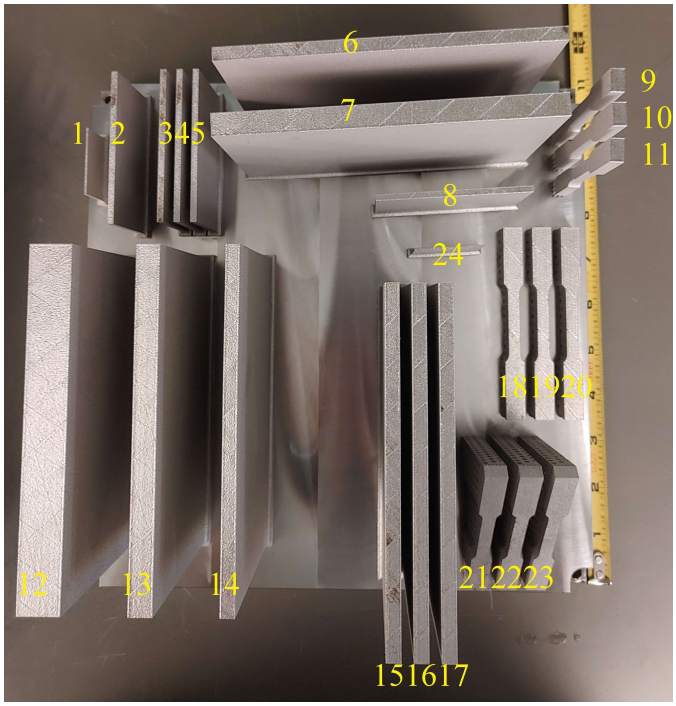

Figure 52.2: First build of 316L stainless steel using baseline parameters on the Mines 3D Systems DMP Flex 350.

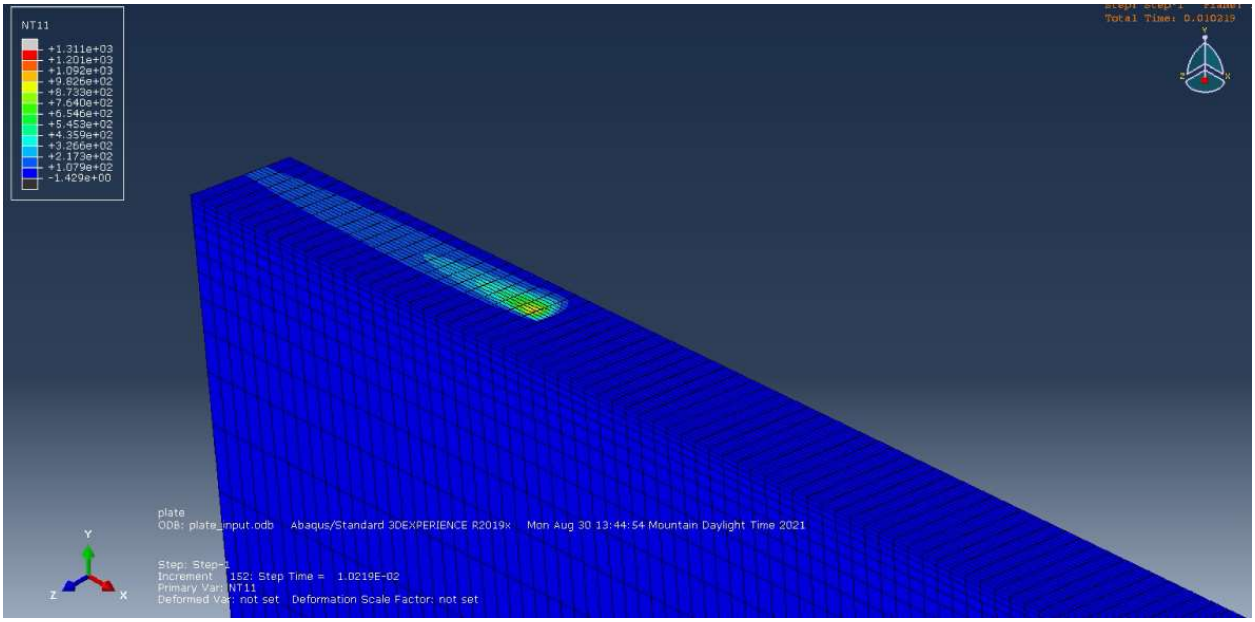

Figure 52.3: Abaqus simulation of plate 1 shown in Figure 52.2 illustrating a moving heat source across the top layer of the build.

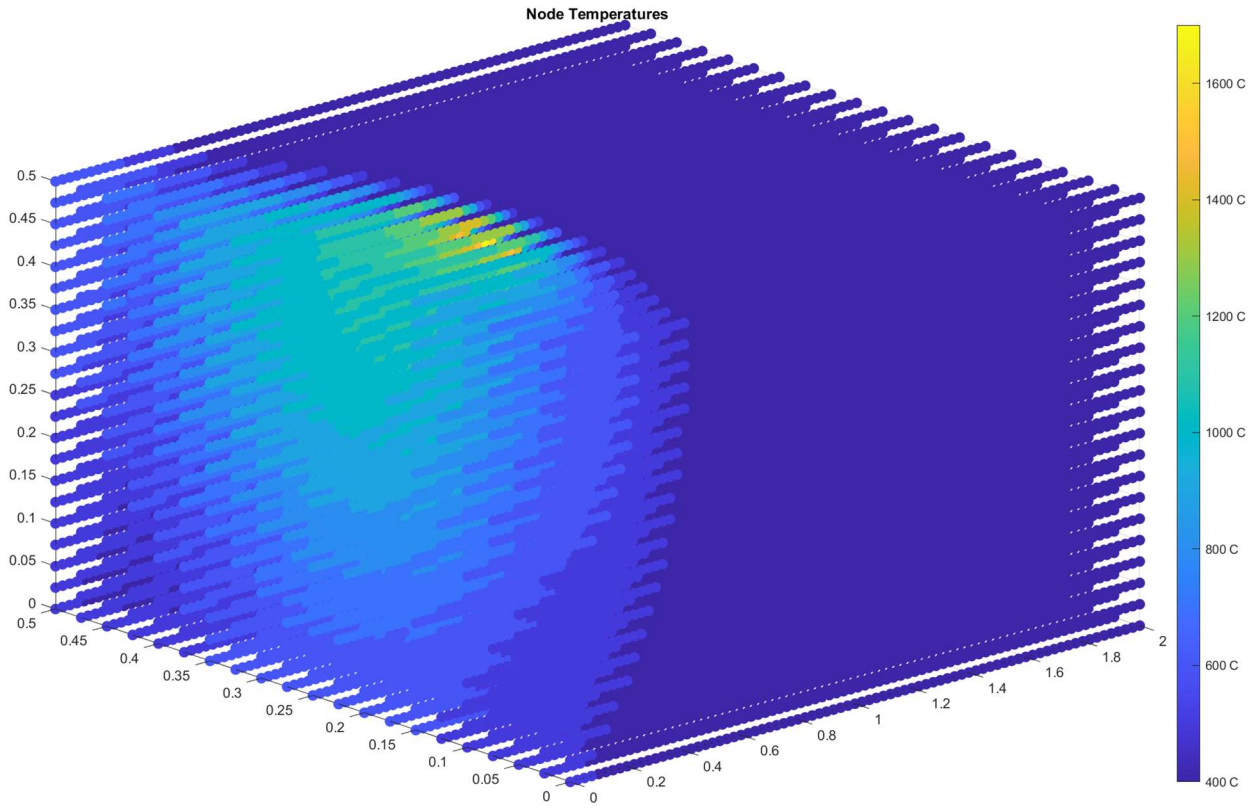

Figure 52.4: Analysis of the Abaqus simulation from Figure 52.3. Each individual dot is a node that records a thermal history allowing G and V to be calculated at different locations throughout the melt pool.